DOI:10.1158/1078-0432.CCR-04-1084

Clinical Cancer Research

Preparation and Biological Evaluation of Copper-64–Labeled Tyr ^{3}-Octreotate Using a Cross-Bridged Macrocyclic Chelator

Jennifer E. Sprague, Yijie Peng, Xiankai Sun, et al.

Clin Cancer Res 2004;10:8674-8682. Published online December 28, 2004.

DOI:10.1158/1078-0432.CCR-04-1084

Preparation and Biological Evaluation of Copper-64–Labeled Tyr^3-Octreotate Using a Cross-Bridged Macrocyclic Chelator

Jennifer E. Sprague,[1] Yijie Peng,[2] Xiankai Sun,[1] Gary R. Weisman,[2] Edward H. Wong,[2] Samuel Achilefu,[1] and Carolyn J. Anderson[1]

[1]Mallinckrodt Institute of Radiology, Washington University School of Medicine, St. Louis, Missouri; and [2]Department of Chemistry, University of New Hampshire, Durham, New Hampshire

ABSTRACT

Purpose: **Somatostatin receptors (SSTr) are expressed on many neuroendocrine tumors, and several radiotracers have been developed for imaging these types of tumors. For this reason, peptide analogues of somatostatin have been well characterized. Copper-64 ($t_{1/2}$ = 12.7 hours), a positron emitter suitable for positron emission tomography (PET) imaging, was shown recently to have improved *in vivo* clearance properties when chelated by the cross-bridged tetraazamacrocycle 4,11-bis(carboxymethyl)-1,4,8,11-tetraazabicyclo(6.6.2)hexadecane (CB-TE2A) compared with 1,4,8,11-tetraazacyclotetradecane-1,4,8,11-tetraacetic acid (TETA).**

Experimental Design: **CB-TE2A and TETA were conjugated to the somatostatin analogue tyrosine-3-octreotate (Y3-TATE) for evaluation of CB-TE2A as a bifunctional chelator of ^{64}Cu. The *in vitro* affinity of each compound for SSTr was determined using a homologous competitive binding assay. *In vivo* characteristics of both radiolabeled compounds were examined in biodistribution and microPET studies of AR42J tumor-bearing rats.**

Results: **Cu-CB-TE2A-Y3-TATE (K_d = 1.7 nmol/L) and Cu-TETA-Y3-TATE (K_d = 0.7 nmol/L) showed similar affinities for AR42J derived SSTr. In biodistribution studies, nonspecific uptake in blood and liver was lower for ^{64}Cu-CB-TE2A-Y3-TATE. Differences increased with time such that, at 4 hours, blood uptake was 4.3-fold higher and liver uptake was 2.4-fold higher for ^{64}Cu-TETA-Y3-TATE than for ^{64}Cu-CB-TE2A-Y3-TATE. In addition, 4.4-times greater tumor uptake was detected with ^{64}Cu-CB-TE2A-Y3-TATE than with ^{64}Cu-TETA-Y3-TATE at 4 hours postinjection. MicroPET imaging yielded similar results.**

Conclusions: **CB-TE2A appears to be a superior *in vivo* bifunctional chelator of ^{64}Cu for use in molecular imaging by PET or targeted radiotherapy due to both improved nontarget organ clearance and higher target organ uptake of ^{64}Cu-CB-TE2A-Y3-TATE compared with ^{64}Cu-TETA-Y3-TATE.**

INTRODUCTION

Extensive studies have been conducted on radiolabeled somatostatin analogues for both imaging and radiotherapy of somatostatin receptor-positive tumors. Modifications to octreotide, a somatostatin analogue, have been evaluated to improve target tissue uptake in somatostatin receptor subtype 2 (SSTr2)-positive tissues; based on these, the octapeptide Tyr^3-octreotate (Y3-TATE) was identified (1, 2). Radiolabeled somatostatin analogues incorporating positron-emitting radionuclides such as ^{64}Cu and ^{68}Ga have been shown to be equivalent or improved SSTr2 tracers for positron emission tomography (PET) imaging of SSTr2-positive tumors compared with ^{111}In-labeled somatostatin analogues for γ scintigraphy (3–5). Copper-64, ^{177}Lu, and ^{90}Y-radiolabeled somatostatin analogues have also shown promise as radiotherapeutic agents for the treatment of SSTr-positive tumors (6–12).

Copper-64 ($t_{1/2}$ = 12.7 hours) is both a positron (β^+; 17.4%, $E_{\beta+max}$ = 656 keV) and β minus (β^-; 39%, $E_{\beta-max}$ = 573 keV) emitter and can be produced in high specific activity on a small biomedical cyclotron (13, 14). The decay characteristics of ^{64}Cu make it suitable for PET imaging as well as radiotherapy when targeted to tumors using monoclonal antibodies or peptides (6, 7, 15–19). Biodistribution and metabolism studies of ^{67}Cu and ^{64}Cu-bifunctional chelator-monoclonal antibodies or peptide conjugates have demonstrated significant dissociation from the bifunctional chelator resulting in transchelation to liver superoxide dismutase (20, 21). For the somatostatin analogue ^{64}Cu-TETA-octreotide (where TETA is 1,4,8,11-tetraazacyclotetradecane-1,4,8,11-tetraacetic acid), this resulted in retention of ^{64}Cu activity in blood, poor liver clearance, and increasing bone marrow uptake over time (7). High blood uptake and retention in the liver reduce imaging sensitivity by increasing background radioactivity levels. High accumulation of ^{64}Cu in the bone marrow may limit the therapeutic dose of $^{64/67}$Cu-bifunctional chelator-peptide due to myelotoxicity (22).

Weisman, Wong, and coworkers (23, 24) have synthesized and characterized a series of copper (II) cross-bridged cyclam complexes that demonstrate improved kinetic stability compared with TETA complexes. Sun *et al.* (25) evaluated the biodistribution of four ^{64}Cu-labeled cross-bridged cyclam complexes in rats and found ^{64}Cu-CB-TE2A (CB-TC2A-4,11-bis(carboxymethyl)-1,4,8,11-tetraazabicyclo[6.6.2]hexadecane)

Received 6/3/04; revised 7/29/04; accepted 8/12/04.
Grant support: NIH Grant R01 CA93375 (E. Wong, G. Weisman, and C. Anderson), R01 CA64475 (C. Anderson), and R21 CA100972 (S. Achilefu). The production of Cu-64 at Washington University School of Medicine is supported by the NCI Grant R24 CA86307. Small animal imaging at Washington University School of Medicine is supported by the NIH Grant 5 R24 CA83060. J. Sprague was supported by the NIH Medical Scientist Training Program Grant T32 GM07200-2 and the Department of Energy Training Grant DE F0101 NE23051.
The costs of publication of this article were defrayed in part by the payment of page charges. This article must therefore be hereby marked *advertisement* in accordance with 18 U.S.C. Section 1734 solely to indicate this fact.
Requests for reprints: Carolyn J. Anderson, Mallinckrodt Institute of Radiology, Washington University School Of Medicine, 510 South Kingshighway Boulevard, Campus Box 8225, St. Louis, MO 63110.

DOI:10.1158/1078-0432.CCR-04-1084

to have the most improved blood, liver, and kidney clearance compared with ^{64}Cu-TETA (26). Transchelation to liver superoxide dismutase was reduced for ^{64}Cu-CB-TE2A compared with ^{64}Cu-TETA in rat metabolism studies (27). These data suggest that CB-TE2A–peptide conjugates may possess improved biodistribution characteristics, making CB-TE2A an attractive bifunctional chelator for attaching ^{64}Cu to peptides for tumor imaging and radiotherapy.

Because Y3-TATE is a well-characterized SSTr2 ligand, this peptide is a good model for evaluating novel bifunctional chelator-peptide conjugates. The AR42J rat pancreatic carcinoma cell line expresses SSTr2 both *in vitro* and *in vivo* (28–31). In these studies we report *in vitro* and *in vivo* characterization of ^{64}Cu-CB-TE2A-Y3-TATE and ^{64}Cu-TETA-Y3-TATE (Fig. 1) in the AR42J tumor model.

MATERIALS AND METHODS

Copper-64 was produced on a CS-15 biomedical cyclotron at Washington University School of Medicine according to published procedures (13). Copper chloride ($CuCl_2$) was purchased from Johnson Matthey (West Deptford, NJ). Trifluoroacetic acid (TFA) was purchased from J.T. Baker (Chicago, IL). 9-Fluorenylmethoxycarbonyl (Fmoc) amino acids were purchased from Novabiochem (San Diego, CA). All of the other chemicals were purchased from Sigma-Aldrich Chemical Co. (St. Louis, MO). All of the solutions were prepared using ultrapure water (18 MΩ-cm resistivity). TLC was performed using Whatman $MKC_{18}F$ reversed-phase plates with 10% ammonium acetate to methanol (30:70) as the mobile phase. Radio-TLC detection was accomplished using a BIOSCAN AR2000 Imaging Scanner (Washington, DC). Analytical reversed-phase high-performance liquid chromatography (HPLC) was performed on a Waters 600E (Milford, MA) chromatography system with a Waters 991 photodiode array detector and an Ortec Model 661 (EG&G Instruments, Oak Ridge, TN) radioactivity detector. HPLC samples were analyzed on a Vydac diphenyl column (4.6 × 100 mm; Hesperia, CA). The mobile phase was H_2O (0.1% TFA; solvent A) and 90% acetonitrile (ACN; 0.1% TFA; solvent B). The gradient consisted of 5% B to 70% B in 20 minutes (1.0 mL/min flow rate). Radioactive samples were counted using a Beckman 8000 automated well-type gamma counter (Fullerton, CA). Electrospray mass spectrometry was accomplished using a Waters Micromass ZQ (Milford, MA).

Male Lewis rats (21-days old, 40–50 g) were purchased from Charles River Laboratories (Boston, MA). The AR42J tumor line was obtained from American Type Culture Collection (ATCC, Rockville, MD).

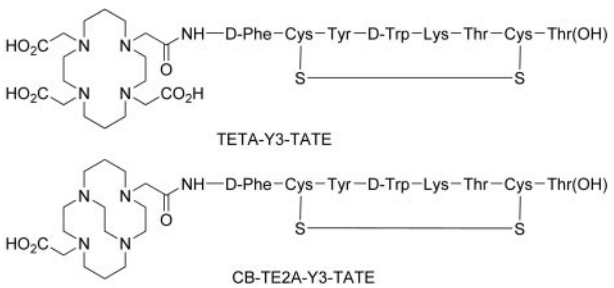

Fig. 1 Structures of TETA-Y3-TATE and CB-TE2A-Y3-TATE.

Synthesis of 4,11-Bis-(carbo-*tert*-butoxymethyl)-1,4,8,11-tetraazabicyclo[6.6.2]hexadecane. 1,4,8,11-Tetraazabicyclo-[6.6.2]hexadecane was prepared as reported previously (24).

Anhydrous sodium carbonate (1.18 g, 11.1 mmol) and t-butyl bromoacetate (2.17 g, 11.13 mmol) were added to a solution of 1,4,8,11-tetraazabicyclo[6.6.2]hexadecane (1.12 g, 4.95 mmol) in acetonitrile (30 mL). The mixture was stirred under N_2 and heated to 50°C for 48 hours. Solvent was then removed under reduced pressure, and residual material was dissolved in 20% aqueous NaOH (20 mL) at ice bath temperature (0–5°C). The aqueous solution was extracted with cold (0–5°C) toluene (3 × 20 mL), combined extracts were dried (anhydrous Na_2SO_4), and solvent was removed under reduced pressure to give an oil, which solidified on standing (2.08 g, 4.58 mmol, 93%): mp 39–40°C; ^{1}H NMR (400 MHz, C_6D_6) δ 1.21–1.46 (m, 4H), 1.40 (s, 18H, $C(CH_3)_3$), 2.22 (ddd, 2H, J = 13.5, 3.9, 1.9 Hz), 2.29 (ddd, 2H, J = 13.1, 4.9, 2.5 Hz), 2.42–2.56 (XX' of AA'XX', 2H, $NCH_AH_XCH_A$·H_X·N cross-bridge), 2.60–2.94 (m, 10H), 3.01 and 3.17 (AB, 4H, J = 16.4 Hz, N-CH_AH_B-CO_2), 3.24–3.40 (AA' of AA'XX', 2H, $NCH_AH_XCH_A$·H_X·N cross-bridge), 3.69 (td, 2H, J = 11.9, 4.2 Hz); ^{13}C NMR (100.5 MHz, C_6D_6) δ 28.10 ($C(CH_3)_3$), 28.20 ($CH_2CH_2CH_2$), 50.87, 53.32, 55.96, 56.31, 57.24, 60.13, 79.67 ($C(CH_3)_3$), 171.08 (*C*=O); IR (KBr) 2976, 2917, 2819, 2784, 1739, and 1728 (C=O), 1477, 1367, 1392, 1323, 1165, 1122 cm^{-1}; HRFABMS, *m/z* $(M+H)^+$ exact mass calculated for $C_{24}H_{47}N_4O_4$: 455.3597; Found: 455.3600 (error 2.5 ppm).

Bis-(Trifluoroacetic Acid) Salt of CB-TE2A. 4,11-Bis-(carbo-*tert*-butoxymethyl)-1,4,8,11-tetraazabicyclo[6.6.2]-hexadecane (1.182 g, 2.600 mmol) was dissolved in a 1:1 (vol:vol) mixture of CF_3CO_2H (TFA) and CH_2Cl_2 (40 mL). The mixture was stirred under N_2 at room temperature for 48 hours. Solvent was removed under reduced pressure to give an oil, which crystallized after removal of residual solvent under vacuum to yield 1.510 g (2.566 mmol, 99%) of product as the di-TFA salt monohydrate: mp 165–169°C; ^{1}H NMR (400 MHz, CD_3CN, CD_2HCN central peak set to 1.94 ppm) δ 1.64–1.74 (dm, 2H, J = 16.8 Hz, $CH_2CH_{eq}H_{ax}CH_2$), 2.18–2.34 (~qm, 2H, J = ~13 Hz, $CH_2CH_{eq}H_{ax}CH_2$), 2.57–2.67 (dm, 2H, J = 13.6 Hz), 2.89–3.14 (m, 12H), 3.31 (td, 2H, J = 13.0, 3.3 Hz), 3.43–3.48 (AA'BB', 4H, NCH_2CH_2N cross-bridge), 3.46 (d, 2H, J = 17.0 Hz, $NCH_AH_XCO_2$), 4.14 (d, 2H, J = 17.0 Hz, $NCH_AH_XCO_2$), (Note: N-*H*/CO_2H fast-exchange signal broadened into baseline. In other spectra, broad signals integrating for up to 4H were observed in the range 8.9–12 ppm); ^{13}C NMR (100.5 MHz, CD_3CN, CD_3CN central peak set to 1.39 ppm) δ 20.63, 48.48, 48.84, 54.35, 56.28, 59.09, 60.81, 172.69 (*C*=O); IR (KBr) 3408, 2960, 2886, 2529, 1723 (C=O), 1433, 1198, 1132, 722 cm^{-1}; Anal Calcd for $C_{16}H_{30}N_4O_4$·2TFA· H_2O: C, 40.82; H, 5.82; N, 9.52. Found: C, 41.14; H, 5.91; N, 9.62.

Synthesis of TETA-Y3-TATE and CB-TE2A-Y3-TATE. Y3-TATE was prepared on solid support by standard Fmoc procedure (32, 33) using an Advanced Chem Tech peptide synthesizer. To facilitate on-board cyclization, acetamidomethyl thiol-protected cysteine was used to introduce the cysteine amino acids (34). After peptide assembly, intramolecular disulfide cyclization was performed on solid support with thallium

DOI:10.1158/1078-0432.CCR-04-1084

trifluoroacetate (23 mg, 42 μmol in 2 mL DMF) for 90 minutes, and the resin was thoroughly washed with DMF. The *N*-terminal Fmoc protecting group was removed from the peptide with 20% piperidine in DMF. The resin was sequentially washed with DCM (2 × 3 mL), methanol (2 × 3 mL), and DCM (2 × 3 mL), and was dried under house vacuum. The peptide-resin was then swollen in DCM (3 mL) for 45 minutes and washed with DMF (3 mL) without drying the resin. CB-TE2A·2TFA salt (39 mg, 68 μmol) was dissolved in DMF (500 μL). To this solution was added diisopropylcarbodiimide (DIC, 8.3 mg, 66 μmol) and DIEA (8.5 mg, 66 μmol), and the solution was stirred for 25 minutes before adding it to the wet peptide-resin. The mixture was gently agitated for 3 hours and filtered. The resin was washed with DCM (95 × 3 mL) and dried under vacuum before cleavage. TETA-Y3-TATE was synthesized as described previously (35).

Both CB-TE2A-TATE and TETA-Y3-TATE were cleaved from the resin with a mixture of TFA/water/thioanisol/phenol (85:5:5:5) for 4 hours and precipitated in cold *t*-butyl methyl ether. The crude peptide conjugates were purified by semi-preparative reverse-phase HPLC using two solvent systems A and B with the gradient elution protocols: 30% to 70% B in 45 minutes at a flow rate of 10 mL/min, where A is 5% CH_3CN in 0.1% aqueous TFA and B is 10% H_2O in 0.1% TFA solution of CH_3CN. Peak detection was at 214 nm with a tunable absorbance detector. The purified compounds (~10% isolated yield) were lyophilized in H_2O/MeCN (3:2) mixture and characterized by analytical HPLC, electrospray mass spectrometry and also by high-resolution mass spectrometry (matrix-assisted laser desorption/ionization) for CB-TE2A-Y3-TATE [*m/z* calculated for $C_{65}H_{92}N_{14}O_{15}S_2$ $(M + H)^+$ = 1373.6386; found 1373.6532].

Preparation of ^{64}Cu-TETA-Y3-TATE and ^{64}Cu-CB-TE2A-Y3-TATE. Radiolabeling of TETA-Y3-TATE with ^{64}Cu(II) was based on methods reported previously (35); here, 0.1 mol/L ammonium acetate (pH 6.5) was used as the reaction solvent. For CB-TE2A-Y3-TATE, 1–15 mCi (37–555 MBq) of ^{64}Cu in 0.1 mol/L ammonium acetate (pH 8.0) was added to 1 to 15 μg of the peptide in 0.1 mol/L ammonium acetate (pH 8.0). The reaction mixture was heated for 1 hour at 95°C. Radiochemical purity for both ^{64}Cu-labeled conjugates was determined by radio-TLC using Whatman MKC18F TLC plates developed with 10% NH_4OAc to methanol ratio (30:70) and was confirmed by radio-HPLC.

Receptor Binding Assays. The affinity of ^{64}Cu-TETA-Y3-TATE or ^{64}Cu-CB-TE2A-Y3-TATE for SSTr2 was measured in AR42J tumor membranes using methods described previously for homologous competitive binding (7). To reduce nonspecific binding, 0.1% BSA was added to the receptor-binding buffer [50 mmol/L Tris-HCl (pH 7.4), 5.0 mmol/L $MgCl_2$ 0.5 μg/mL aprotinin, 200 μg/mL bacitracin, 10 μg/mL leupeptin, and 10 μg/mL pepstatin A]. The competing ligands, ^{nat}Cu-TETA-Y3-TATE or ^{nat}Cu-CB-TE2A-Y3-TATE, were prepared with high-purity natural copper chloride ($CuCl_2$) using the procedure described above for preparation of the ^{64}Cu-labeled peptides. Complex formation was confirmed by HPLC and electrospray mass spectrometry. IC_{50} values were determined according to published methods (7) using the Millipore MultiScreen Assay system (Bedford, MA). Data analysis was performed using GraphPad PRISM (San Diego, CA) for non-linear regression of homologous competitive binding curves with ligand depletion.

Internalization Assay. The procedure for the cellular internalization assay was based on the method published by Wang *et al.* (36). Forty-eight hours before each assay, AR42J cells (1.9×10^6 cells per well) were seeded in 6-well BD Primaria plates (BD Biosciences, Bedford, MA) containing F12K media supplemented with 2 mmol/L L-glutamine, 1.5 g/L sodium bicarbonate, and 20% fetal bovine serum; cells were incubated at 37°C in a humidified 5% CO_2 atmosphere. Cells were washed twice with HBSS, and then 1 mL of F12K supplemented media was added to each well. To block specific binding, at each time point 3 of 6 wells were incubated 5 minutes at room temperature with 2 μg Y3-TATE. To each well was added ^{64}Cu-CB-TE2A-Y3-TATE (specific activity = 0.23 mCi/μg) or ^{64}Cu-TETA-Y3-TATE (specific activity = 0.23 mCi/μg) to a final concentration of 4.0 nmol/L of each radiotracer. Cells were incubated at 37°C. At each time point, surface-bound fractions were collected as described by Wang *et al.* (36). Internalized radioactivity was collected by lysing the cells in 0.5% SDS. Total protein concentration in the cell lysate was determined using the BCA Protein Assay (Pierce Biotechnology, Rockford, IL). Internalized and surface bound fractions were expressed as fmol radiotracer/mg protein.

Animal Model. All of the animal experiments were performed in compliance with the Guidelines for the Care and Use of Research Animals established by Washington University's Animal Studies Committee. AR42J tumors (Mallinckrodt, Inc., St. Louis, MO, passage 36) were implanted in the left leg of male Lewis rats (21 days old) and maintained by serial passage in animals as described previously (37). Tumors were allowed to grow 10 to 14 days by which time tumors achieved a solid palpable mass.

Animal Biodistribution Studies. The ^{64}Cu-labeled peptide conjugates (40 μCi, 140 ng ^{64}Cu-TETA-Y3-TATE; 50 μCi, 170 ng ^{64}Cu-CB-TE2A-Y3-TATE) were injected i.v. via the tail vein into AR42J tumor-bearing rats. Tissue biodistribution data were obtained at 1, 4, and 24 hours after injection according to methods described previously (35).

To examine *in vivo* uptake specificity, additional AR42J tumor-bearing Lewis rats were injected with ^{64}Cu-TETA-Y3-TATE (50 μCi, 170 ng) or ^{64}Cu-CB-TE2A-Y3-TATE (10 μCi, 35 ng) via the tail vein with or without coinjection of 150 μg of Y3-TATE (CS Bio, San Carlos, CA). Tissue biodistributions were obtained.

Blood Clearance Studies. AR42J tumor-bearing rats were anesthetized with 1% to 2% isoflurane for the duration of the study. Catheters were placed in the femoral artery and vein. The femoral artery catheter was used to administer ^{64}Cu-TETA-Y3-TATE (140 μCi, 165 ng) or ^{64}Cu-CB-TE2A-Y3-TATE (160 μCi, 190 ng). Blood samples (5 μ L) were drawn through the femoral vein catheter in capillary tubes between 15 seconds and 1 hour after injection. At 1 hour, a biodistribution study was performed as described above.

microPET Imaging. PET imaging was performed on a microPET-R4 scanner (Concorde Microsystems, Knoxville, TN). Imaging studies were carried out on male Lewis rats bearing AR42J tumors. Four rats were i.v. injected via the tail vein with ^{64}Cu-TETA-Y3-TATE (0.73 mCi, 2.7 μg) or ^{64}Cu-

DOI:10.1158/1078-0432.CCR-04-1084

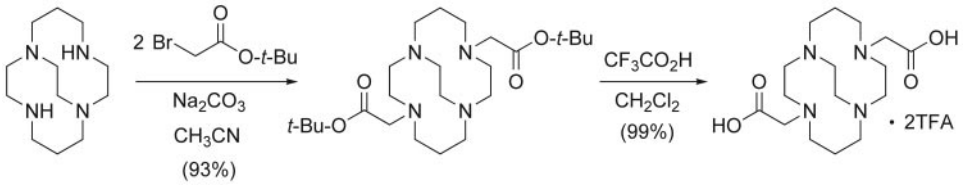

Fig. 2 Schematic for the synthesis of CB-TE2A.

CB-TE2A-Y3-TATE (0.77 mCi, 3.5 μg). At 1, 4, and 24 hours after injection, rats were anesthetized with 1% to 2% isoflurane, positioned supine, immobilized, and imaged in two bed positions. Immediately after imaging, a biodistribution study was performed on each rat as described above. Tumor, kidney, and liver standard uptake values {(nCi/ml) × [weight (g)/injected dose (nCi)]} of ^{64}Cu-activity were generated by measuring regions of interest that encompassed the entire organ from the microPET images of AR42J tumor-bearing Lewis rats.

Statistical Methods. All of the data are presented as mean ± SD or mean (95% confidence interval). For statistical classification, a Student *t* test (two-tailed, unpaired) was performed using GraphPad PRISM (San Diego, CA). *P*s < 0.05 were considered significant.

RESULTS

Synthesis of CB-TE2A. The chelating agent CB-TE2A was synthesized as shown in Fig. 2. The parent cross-bridged cyclam [1,4,8,11-tetraazabicyclo[6.6.2]-hexadecane] was dialkylated with t-butyl bromoacetate to give the conveniently handled and quantified pendant-arm bis(t-butyl ester) in excellent yield (93%). This synthetic intermediate was cleanly and quantitatively deprotected with trifluoroacetic acid in dichloromethane to give CB-TE2A as the bis(trifluoroacetic acid) salt, which was used for the subsequent bioconjugation. This preparation of CB-TE2A is an improvement over our route published previously involving the intermediacy of the bis(ethyl ester; ref. 24).

Synthesis of CB-TETA-Y3-TATE and TE2A-Y3-TATE. The peptide Y3-TATE was first assembled on a Wang resin by standard Fmoc solid phase peptide synthesis. A one-pot coupling method was used to introduce CB-TE2A to the peptide by using DIC, which forms both intramolecular and intermolecular anhydrides. The activated intermediate can react with the free amino group of the peptide to form the amide linkage while simultaneously generating a free unactivated carboxyl group. Additionally, the use of low loading resins (<0.4 mmol reactive function/g resin) prevents the dimerization of possible oligomeric acid anhydrides.

A solid-phase method was used to conjugate TETA to Y3-TATE as a solution phase reaction yielded an intractable mixture of products. To solubilize the chelator, minimize hydrolysis of activated carboxyl function, and prevent complete shrinking of the resin, a mixture of DMSO and water in the ratio of 1:100 (v/v) was used. A low-load Wang resin (<0.4 mmol/g resin) was used for the coupling reaction. *N,N,N′,N′*-Tetramethyl-O-(1H-benzotriazol-1-yl)uronium hexafluorophosphate was used as the coupling reagent to give the desired compound in ~ 10% yield (100% HPLC purity).

Preparation of ^{64}Cu-TETA-Y3-TATE and ^{64}Cu-CB-TE2A-Y3-TATE. Initial radiolabeling experiments of CB-TE2A-Y3-TATE with ^{64}Cu in NH_4OAc (pH 7.0) at 60°C resulted in <40% radiochemical yield (decay corrected) after 4 hours without purification. Raising the temperature to 95°C reduced the reaction time to 2 hours with >95% radiochemical yield (decay corrected) and eliminated the need for any purification steps. This was desirable as including a SepPak purification step reduced the yield by 40% to 50%. The labeling procedure was additionally modified by raising the reaction pH from 7.0 to 8.0. Changing the pH reduced the reaction time to 1 hour without affecting radiochemical yield and improved maximal specific activity from 1.3 mCi/μg to 5.1 mCi/μg. Radiochemical purity of ^{64}Cu-CB-TE2A-Y3-TATE and ^{64}Cu-TETA-Y3-TATE was >95% as determined by radio-TLC and radio-HPLC. Radiolabeled peptides were used immediately or stored overnight at 4°C. Radiochemical purity was not reduced by overnight storage as determined by radio-TLC.

Receptor Binding Assay. A homologous competitive binding assay was performed using AR42J tumor membranes bearing SSTr2. ^{64}Cu-CB-TE2A-Y3-TATE and ^{64}Cu-TETA-Y3-TATE were challenged with increasing concentrations of their respective natural isotopic abundance copper complexes. The IC_{50} values were determined to be 0.8 nmol/L (0.6–1.3 nmol/L, 95% confidence interval, CI) and 2.3 nmol/L (1.7–3.2 nmol/L, 95% CI) for ^{nat}Cu-TETA-Y3-TATE and ^{nat}Cu-CB-TE2A-Y3-TATE, respectively (Fig. 3). k_d was calculated to be 0.7 nmol/L (0.5–1.1 nmol/L, 95% CI) for the TETA conjugate and 1.7 nmol/L (1.2–2.4 nmol/L, 95% CI) for the cross-bridged conjugate. These results suggest that Cu-TETA-Y3-TATE and Cu-CB-TE2A-Y3-TATE have similar binding affinities for SSTr in AR42J cell membranes. B_{max} was determined to be 192 fmol/mg (123–262 fmol/mg, 95% CI) for ^{nat}Cu-TETA-Y3-TATE and 1596 fmol/mg (1088–2103 fmol/mg, 95% CI) for ^{nat}Cu-CB-TE2A-Y3-TATE.

Internalization Assay. AR42J cells in culture demonstrated time-dependent internalization of both ^{64}Cu-CB-TE2A-Y3-TATE and ^{64}Cu-TETA-Y3-TATE that was readily blocked by Y3-TATE in the media (Fig. 4*A*). Near-linear internalization over time was observed for ^{64}Cu-CB-TE2A-Y3-TATE to 60 minutes (slope = 21.3 ± 2.0, y-intercept = 516 ± 82 fmol/mg, $r^2 = 0.95$); the amount of radiotracer internalized at later time points showed no significant change. The nonzero y-intercept of cross-bridged complex suggests a rapid early internalization phase before 15 minutes followed by a slower internalization phase to 1 hour. ^{64}Cu-TETA-Y3-TATE uptake was significantly less than ^{64}Cu-CB-TE2A-Y3-TATE at 15 ($P = 0.0002$), 30 ($P < 0.0001$), and 60 ($P = 0.0025$) minutes. ^{64}Cu-TETA-Y3-

DOI:10.1158/1078-0432.CCR-04-1084

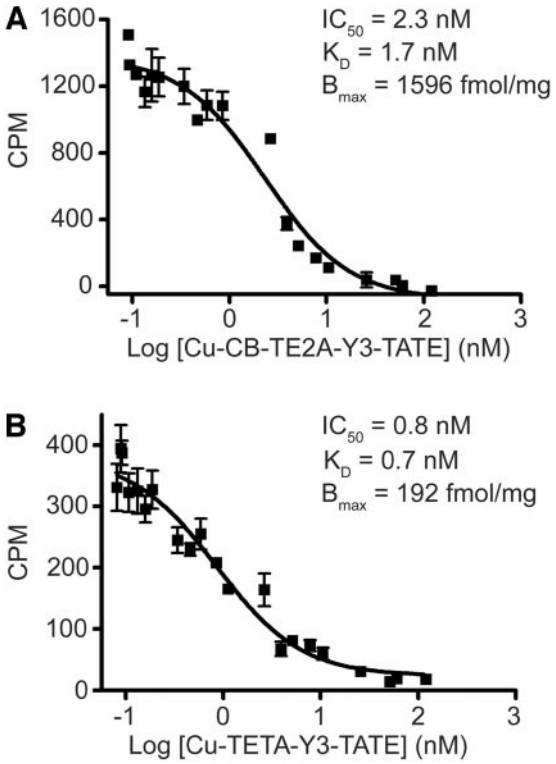

Fig. 3 *In vitro* binding affinity of ^{64}Cu-CB-TE2A-Y3-TATE (*A*) and ^{64}Cu-TETA-Y3-TATE (*B*) for SSTr2 harvested from AR42J rat pancreatic tumor cell membranes was determined using a homologous competitive binding assay. Specific binding was blocked with increasing doses of ^{nat}Cu-CB-TE2A-Y3-TATE (*A*) and ^{nat}Cu-TETA-Y3-TATE (*B*), respectively ($n = 3$; *bars,* ±SE).

TATE internalization increased linearly to 120 minutes (slope = 18.0 ± 1.0, y-intercept = −47.8 ± 67.6 fmol/mg, $r^2 = 0.97$). There was no difference between TETA and CB-TE2A peptide-conjugate internalization at 120 and 240 minutes. By 240 minutes, 48.1 ± 1.4% dose/mg protein ^{64}Cu-CB-TE2A-Y3-TATE and 47.1 ± 2.3% dose/mg protein ^{64}Cu-TETA-Y3-TATE was internalized.

The surface-bound fraction of radiotracer was also quantified (Fig. 4*B*). For both conjugates, cell surface-associated activity was specifically blocked by Y3-TATE. The amount of ^{64}Cu-CB-TE2A-Y3-TATE bound to the cell surface was significantly higher than ^{64}Cu-TETA-Y3-TATE at all of the time points ($P \leq 0.009$) except 120 minutes. For ^{64}Cu-CB-TE2A-Y3-TATE, the surface-bound activity fell slightly over time. At 240 minutes, the surface-bound fraction was 7.88 ± 0.02% dose/mg protein for ^{64}Cu-CB-TE2A-Y3-TATE and 7.19 ± 0.59% dose/mg protein for ^{64}Cu-TETA-Y3-TATE.

Animal Biodistribution Studies. The tumor and tissue uptakes of ^{64}Cu in AR42J tumor-bearing rats are shown in Fig. 5. Both ^{64}Cu-TETA-Y3-TATE and ^{64}Cu-CB-TE2A-Y3-TATE demonstrated rapid blood clearance (0.242 ± 0.071%ID/g for ^{64}Cu-TETA-Y3-TATE at 1 hour, 0.127 ± 0.015%ID/g for ^{64}Cu-CB-TE2A-Y3-TATE at 1 hour). By 24 hours, the ^{64}Cu activity in blood had fallen to <60% of the 1-hour activity for ^{64}Cu-TETA-Y3-TATE and to 11% of the 1-hour activity for ^{64}Cu-CB-TE2A-Y3-TATE resulting in 10-fold higher blood activity at 24 hours for ^{64}Cu-TETA-Y3-TATE ($P < 0.0001$). In addition, liver uptake at all of the time points was significantly higher for ^{64}Cu-TETA-Y3-TATE than for ^{64}Cu-CB-TE2A-Y3-TATE ($P < 0.003$). Initially (1 hour) there was 1.8 times greater activity in the kidneys for ^{64}Cu-TETA-Y3-TATE than for ^{64}Cu-CB-TE2A-Y3-TATE ($P < 0.03$). However, the ^{64}Cu-TETA-Y3-TATE activity in the kidneys was reduced by 74% at 24 hours compared with only a 36% reduction in ^{64}Cu-CB-TE2A-Y3-TATE kidney activity over the same period. This resulted in 1.3 times higher uptake of ^{64}Cu-CB-TE2A-Y3-TATE at 24 hours compared with ^{64}Cu-TETA-Y3-TATE ($P < 0.01$).

In a separate study, blocking specific uptake at 1 hour after injection by coinjection of Y3-TATE resulted in a significant increase in ^{64}Cu activity uptake in nontarget organs for ^{64}Cu-CB-TE2A-Y3-TATE (blood = 0.179 ± 0.029% ID/g, blood blocked = 0.382 ± 0.053% ID/g; liver = 0.401 ± 0.065% ID/g, liver blocked = 0.837 ± 0.254% ID/g; kidney = 2.917 ± 0.474% ID/g, kidney blocked = 5.746 ± 0.340% ID/g; $P < 0.02$). This may be due to a general increase in bioavailability of this ^{64}Cu-labeled peptide when coinjected with Y3-TATE to block receptor-mediated uptake. There was no significant increase in nonspecific uptake of ^{64}Cu-TETA-Y3-TATE with a blocking dose of Y3-TATE (data not shown).

At 1 hour after injection there was no difference in ^{64}Cu uptake in bone marrow uptake between the two ^{64}Cu-labeled

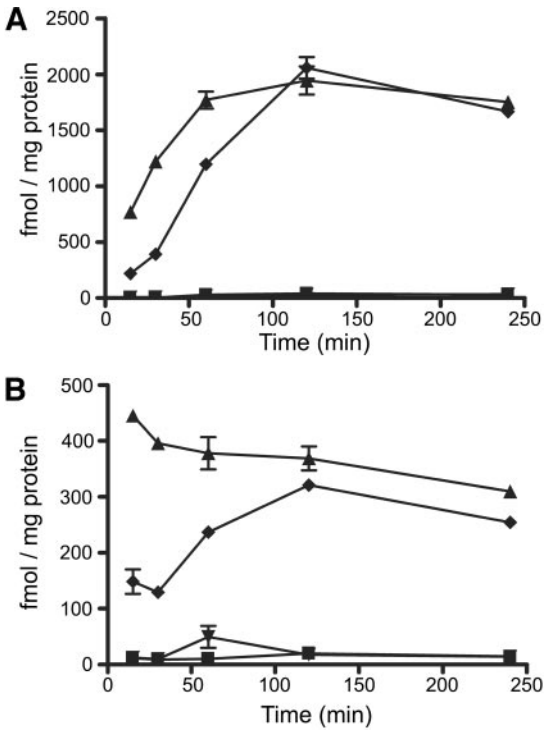

Fig. 4 AR42J cell uptake studies of ^{64}Cu-CB-TE2A-Y3-TATE (▲) and ^{64}Cu-TETA-Y3-TATE (♦). Both internalized (*A*) and surface-bound (*B*) fractions of radioactivity were determined. Cell uptake was blocked by addition of 2 μg Y3-TATE to the incubation media (blocked ^{64}Cu-CB-TE2A-Y3-TATE (■), blocked ^{64}Cu-TETA-Y3-TATE (▼); $n = 3$ for each data point; *bars,* ±SE).

DOI:10.1158/1078-0432.CCR-04-1084

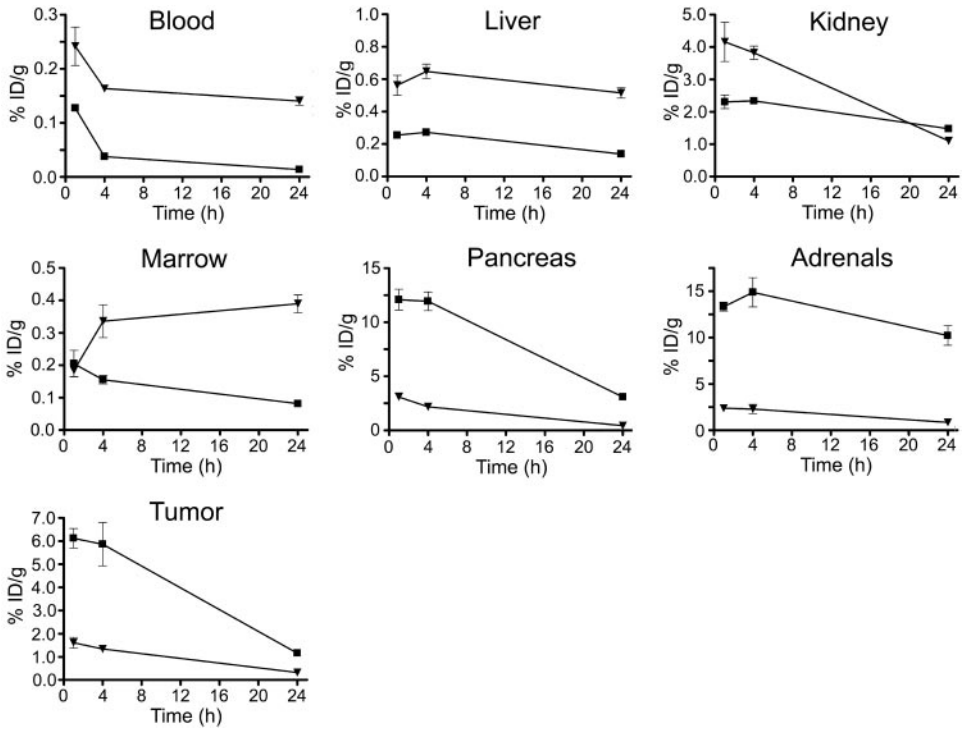

Fig. 5 Biodistribution comparing ^{64}Cu-CB-TE2A-Y3-TATE and ^{64}Cu-TETA-Y3-TATE *in vivo*. Uptake in selected organs of ^{64}Cu-CB-TE2A-Y3-TATE (50 μCi, 170 ng; ■) and ^{64}Cu-TETA-Y3-TATE (40 μCi, 140 ng; ▼) determined by biodistribution studies in AR42J pancreatic tumor-bearing Lewis rats ($n = 4$; *bars,* ±SE). All of the data were decay corrected. Note differences in *Y*-axis scales.

peptide conjugates (Fig. 5). However, at later time points, the marrow uptake of ^{64}Cu-TETA-Y3-TATE increased such that the 24-hour uptake was 212% the 1-hour uptake. In contrast, the marrow activity for ^{64}Cu-CB-TE2A-Y3-TATE decreased to 39.5% the 1-hour uptake at 24 hours. Thus, by 24 hours the marrow uptake of ^{64}Cu-TETA-Y3-TATE was 4.7-fold higher than ^{64}Cu-CB-TE2A-Y3-TATE ($P < 0.0001$).

The uptakes for ^{64}Cu-CB-TE2A-Y3-TATE in SSTr-positive tumor, pancreas, and adrenal gland were significantly higher than for ^{64}Cu-TETA-Y3-TATE at all of the time points ($P < 0.004$; Fig. 5). For both ^{64}Cu-labeled conjugates, the activity did not change significantly from 1 to 4 hours after injection, suggesting that ^{64}Cu was retained in the tumor for at least 4 hours. Copper-64 activity uptake in the tumor cleared over time (18.9% of 1-hour activity in the tumor at 24 hours for ^{64}Cu-CB-TE2A-Y3-TATE; 20.1% of 1-hour activity in the tumor at 24 hours for ^{64}Cu-TETA-Y3-TATE). Uptake of ^{64}Cu-CB-TE2A-Y3-TATE in adrenals and pancreas was >90% blocked by coinjection of unlabeled Y3-TATE (adrenals = 9.112 ± 2.890% ID/g, adrenals blocked = 0.374 ± 0.056% ID/g; pancreas = 5.841 ± 1.217% ID/g, pancreas blocked = 0.371 ± 0.031) indicating specific targeting to SSTr-positive tissues ($P < 0.001$). In tumors, specific uptake was only reduced by 66% for ^{64}Cu-CB-TE2A-Y3-TATE (tumor = 2.408 ± 0.434% ID/g, tumor blocked = 0.823 ± 0.062% ID/g; $P = 0.0004$) and 74% for ^{64}Cu-TETA-Y3-TATE (tumor = 1.613 ± 0.471% ID/g; tumor blocked = 0.422 ± 0.141% ID/g; $P = 0.003$). This might be attributable to necrosis in the tumor that could result in some nonspecific uptake due to poor tumor clearance.

The tumor to blood ratio at 4 hours for ^{64}Cu-CB-TE2A-Y3-TATE was 156 ± 55; for ^{64}Cu-TETA-Y3-TATE the tumor to blood ratio was 8.2 ± 1.6 ($P < 0.001$). Similarly, the tumor to muscle ratio at 4 hours was significantly higher for ^{64}Cu-CB-TE2A-Y3-TATE (243 ± 85) than for ^{64}Cu-TETA-Y3-TATE (19.6 ± 4.7; $P = 0.0003$).

To demonstrate that the higher specific uptake with ^{64}Cu-CB-TE2A-Y3-TATE compared with ^{64}Cu-TETA-Y3-TATE was not due to increased bioavailability of this compound, blood levels of both radiotracers were monitored for 1 hour after injection (data not shown). For the two compounds, peak blood activity levels (<1 minute after injection) were not significantly different ($P = 0.08$). By 5 minutes after injection, the blood level for both compounds was reduced to ~25% of the peak level. At 60 minutes after injection, blood radioactivity uptake had cleared to <5% maximum blood levels for both compounds. Thus, no differences in blood clearance over the first hour were detected for ^{64}Cu-CB-TE2A-Y3-TATE and ^{64}Cu-TETA-Y3-TATE, and no significant differences in blood radiotracer levels were found at any time point. This suggests equivalent bioavailability for ^{64}Cu-CB-TE2A-Y3-TATE and ^{64}Cu-TETA-Y3-TATE.

MicroPET Images. Fig. 6*A* shows the projection microPET images of AR42J tumor-bearing rats 4 hours after injection of ^{64}Cu-CB-TE2A-Y3-TATE (left) and ^{64}Cu-TETA-Y3-TATE (right). Imaging was performed at 1, 4, and 24 hours after injection. Prominent uptake was observed in the liver and kidneys of all of the animals. Measuring standard uptake values allows a quantitative comparison between microPET images. Standard uptake values for liver, kidneys, and tumor were determined at all of the time points ($n = 2$ rats; Fig. 6*B* and *C*). Liver uptakes were similar for the two radiolabeled conjugates

DOI:10.1158/1078-0432.CCR-04-1084

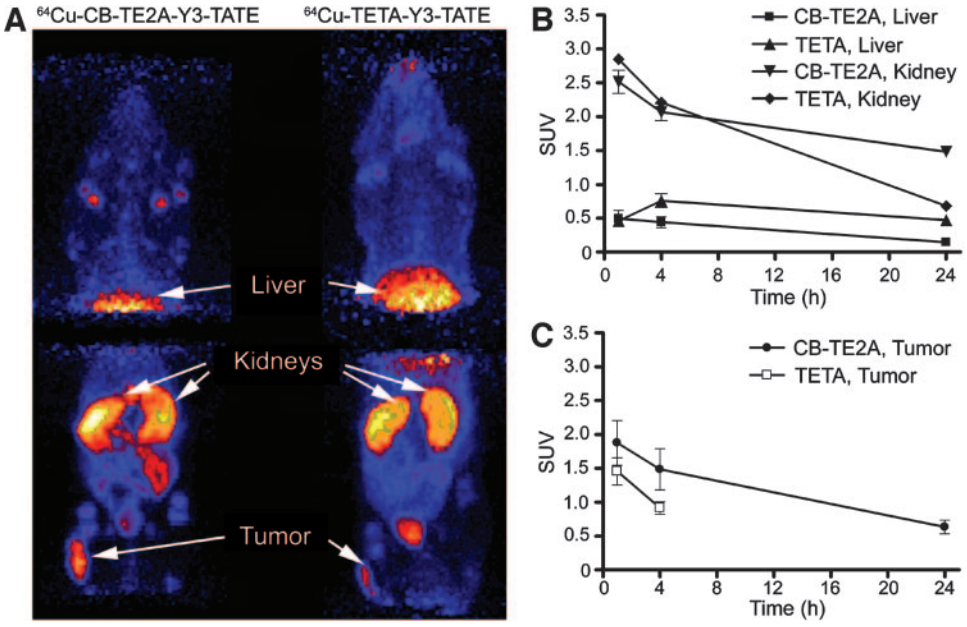

Fig. 6 MicroPET projection images of AR42J tumor bearing rats at 4 hours after injection of ^{64}Cu-CB-TE2A-Y3-TATE and ^{64}Cu-TETA-Y3-TATE. Rats were imaged in two bed positions at 1, 4, and 24 hours after administration of ^{64}Cu-CB-TE2A-Y3-TATE (0.774 mCi, 3.5 μg; *left*) or ^{64}Cu-TETA-Y3-TATE (0.727 mCi, 2.7 μg; *right; A*). Liver, kidney (*B*), and tumor (*C*) ^{64}Cu activity uptake at 1, 4, and 24 hours after administration of ^{64}Cu-CB-TE2A-Y3-TATE or ^{64}Cu-TETA-Y3-TATE. Standard uptake values were calculated by measuring the activity in regions of interest from microPET images of AR42J pancreatic tumor-bearing Lewis rats ($n = 2$; *bars,* ±SE).

at 1 hour, but diverged at later time points rising to 160% of the 1-hour value at 4 hours for ^{64}Cu-TETA-Y3-TATE, whereas liver activity for ^{64}Cu-CB-TE2A-Y3-TATE did not change significantly over this period. By 24 hours after injection, the liver uptake of ^{64}Cu-TETA-Y3-TATE is 3-fold higher than that of ^{64}Cu-CB-TE2A-Y3-TATE ($P < 0.02$). Renal uptake of ^{64}Cu-CB-TE2A-Y3-TATE is only reduced by 41% over 24 hours compared with 76% for ^{64}Cu-TETA-Y3-TATE, which resulted in higher uptake of ^{64}Cu-CB-TE2A-Y3-TATE at 24 hours than of ^{64}Cu-TETA-Y3-TATE. These imaging results are consistent with biodistribution data (Fig. 5*A*).

Standard uptake values were also determined for tumors imaged by microPET with the ^{64}Cu-radiolabeled conjugates (Fig. 6*C*). At all of the time points, ^{64}Cu-CB-TE2A-Y3-TATE had a higher tumor uptake than ^{64}Cu-TETA-Y3-TATE. No tumor uptake was detectable above background by microPET for ^{64}Cu-TETA-Y3-TATE at 24 hours.

DISCUSSION

Copper-64 has been shown to dissociate from TETA and TETA-conjugates and to undergo transchelation to superoxide dismutase in rat liver in biodistribution and metabolism studies (7, 20, 21, 27). The cross-bridged cyclam, CB-TE2A, has demonstrated improved *in vitro* kinetic stability as well as a reduction of *in vivo* transchelation (25, 27, 38). These studies suggest that CB-TE2A is an enhanced chelator compared with TETA for labeling ^{64}Cu for *in vivo* imaging and therapy.

Similar binding affinities for SSTr prepared from AR42J tumor membranes were determined for ^{64}Cu-TETA-Y3-TATE and ^{64}Cu-CB-TE2A-Y3-TATE (Fig. 3). However, there was a significant difference in the B_{max} values measured for the TETA (192 fmol/mg) and CB-TE2A (1551 fmol/mg) conjugates. This might be attributed to a broader specificity for ^{64}Cu-CB-TE2A-Y3-TATE binding to SSTr than for ^{64}Cu-TETA-Y3-TATE. Although AR42J tumors express SSTr2, these tumor cells have also been shown to express SSTr1, SSTr3, and SSTr5 (31). Reubi *et al.* (39) demonstrated that relatively small changes in a radiolabeled peptide, such as changing the chelator, can markedly change the SSTr binding profile of somatostatin analogues. The data reported here suggest that the change from Cu(II)-TETA to Cu(II)-CB-TE2A, *i.e.,* from *trans-* to *cis*-folded coordination geometry (24, 25), does not inhibit peptide interactions with SSTr2 and may improve tumor uptake by binding to other SSTr subtypes. This hypothesis is supported by cell internalization studies, where at early time points, the surface-bound levels of ^{64}Cu-CB-TE2A-Y3-TATE were significantly higher than for ^{64}Cu-TETA-Y3-TATE. In addition, ^{64}Cu-CB-TE2A-Y3-TATE showed more rapid internalization kinetics than ^{64}Cu-TETA-Y3-TATE. Thus, ^{64}Cu-CB-TE2A-Y3-TATE was predicted to have improved specific uptake in target tissues compared with ^{64}Cu-TETA-Y3-TATE.

In vivo, the ^{64}Cu-labeled CB-TE2A conjugate demonstrated greater SSTr-mediated uptake in SSTr-positive tissues compared with the TETA conjugate (Fig. 5). Higher uptake in SSTr-specific tissues for CB-TE2A could not be attributed to differences in bioavailability of the two radiotracers as determined by 1-hour blood clearance profiles. However, both adrenals and pancreas have been shown to express multiple SSTr subtypes including SSTr2 (40, 41); broadening of subtype specificity with Cu-CB-TE2A-Y3-TATE could contribute to higher specific uptake in these organs compared with the TETA conjugate. The more rapid internalization kinetics of the cross-bridged conjugate *in vitro* likely also contributes to the increase in specific uptake observed *in vivo*.

Similar fractions of 1-hour uptake washed out of AR42J tumors by 24 hours for both compounds despite proposed differences in *in vivo* chelate stability. After SSTr/somatostatin analogue complexes are endocytosed, both receptors and ana-

DOI:10.1158/1078-0432.CCR-04-1084

logues are recycled to the cell surface, and the analogues can be reinternalized (42). Because both TETA and CB-TE2A conjugates show similar affinity for SSTr from AR42J cells, it is reasonable to assume that both would be recycled to the same extent regardless of chelate stability.

There was greater accumulation of ^{64}Cu-TETA-Y3-TATE in nontarget tissues such as liver, blood, and marrow compared with ^{64}Cu-CB-TE2A-Y3-TATE; this was increasingly evident at later time points. Higher blood and liver uptake and increasing marrow uptake suggest that ^{64}Cu dissociates from the TETA peptide conjugate to a greater extent than from the CB-TE2A peptide conjugate *in vivo* (21). Differences in nontarget tissue biodistribution likely reflect differences in ^{64}Cu-chelate stability and clearance between ^{64}Cu-CB-TE2A-Y3-TATE and ^{64}Cu-TETA-Y3-TATE.

The *in vivo* behavior of ^{64}Cu-TETA-Y3-TATE in a CA20948 tumor-bearing rat model was described previously by Lewis *et al.* (1). In the current study we report lower target tissue uptake and greater nontarget organ uptake than was found previously (1). The CA20948 rat pancreatic carcinoma model uses older rats than required for AR42J tumors (1, 37). Immature rats may metabolize ^{64}Cu-TETA-Y3-TATE differently from older rats, resulting in the observed differences in biodistribution.

Copper-64 activity was retained in the kidney 24 hours after administration of ^{64}Cu-CB-TE2A-Y3-TATE, whereas ^{64}Cu-TETA-Y3-TATE showed much greater clearance from the kidney (Fig. 5). Differences in renal uptake and excretion may be due to the charge differences of these two conjugates; Cu(II)-TETA-Y3-TATE has a net charge of -1 on the entire conjugate, whereas Cu(II)-CB-TE2A-Y3-TATE is predicted to have a $+1$ charge. Several studies have investigated the effect of charge on kidney uptake of both ^{64}Cu- and ^{111}In-labeled compounds (20, 26, 43). Indium-111-DTPA-conjugated peptides are retained in the kidney after reabsorption by renal tubular cells and lysosomal proteolysis (44, 45). Renal retention of ^{111}In activity was greatest for positively charged peptide conjugates and lowest for negatively charged ones (43). A similar charge effect was seen for ^{64}Cu-labeled azamacrocycles (26). Blocking cationic binding sites in the kidney with D- or L-lysine reduced kidney uptake of ^{111}In-DTPA-D-Phe^{1}-octreotide (46, 47). We suggest that renal uptake of ^{64}Cu-CB-TE2A-Y3-TATE may be blocked by coadministration of lysine. Modification of the CB-TE2A backbone by addition of a carboxylate arm may improve the biodistribution characteristics of ^{64}Cu-CB-TE2A-Y3-TATE by changing the net charge from positive to either neutral or negative. In addition, a cross-bridged chelator with two carboxylates available for complexation may increase the *in vivo* stability of the conjugate relative to ^{64}Cu-CB-TE2A-Y3-TATE resulting in additional improvements in the biodistribution.

In summary, ^{64}Cu-CB-TE2A-Y3-TATE was evaluated for microPET imaging of SSTr-positive tumors in a tumor-bearing rat model. These data suggest that CB-TE2A is a superior chelator for ^{64}Cu compared with TETA, due to improved liver and blood clearance, resulting in higher tumor to tissue ratios. Changing the chelator also increased tumor detection sensitivity by PET for ^{64}Cu-CB-TE2A-Y3-TATE compared with ^{64}Cu-TETA-Y3-TATE. Modifications to CB-TE2A to reduce the net positive charge of the Cu(II) complex may additionally improve the biodistribution. The development of radiopharmaceuticals radiolabeled with ^{64}Cu is a growing area of research. The cross-bridged chelator CB-TE2A represents a highly attractive method for stable complexing of ^{64}Cu to a wide variety of biological molecules. ^{64}Cu-CB-TE2A-Y3-TATE has great potential as a clinical PET radiopharmaceutical for imaging neuroendocrine tumors.

ACKNOWLEDGMENTS

The authors acknowledge Todd A. Perkins and Deborah Sultan for production of ^{64}Cu; Susan Adams, Laura Meyer, Lynne A. Jones, Nicole Fettig, and John Engelbach for their excellent technical assistance; and Jerrel Rutlin and Chih-Hsien Chang for help with microPET data analysis.

REFERENCES

1. Lewis JS, Lewis MR, Srinivasan A, et al. Comparison of four 64-Cu-labeled Somatostatin analogues in vitro and in a tumor-bearing rat model: evaluation of new derivatives for positron emission tomography imaging and targeted radiotherapy. J Med Chem 1999;42:1341–7.

2. de Jong M, Breeman W, Bakker W, et al. Comparison of (111)In-labeled somatostatin analogues for tumor scintigraphy and radionuclide therapy. Cancer Res 1998;58:437–41.

3. Anderson CJ, Dehdashti F, Cutler PD, et al. Copper-64-TETA-octreotide as a PET imaging agent for patients with neuroendocrine tumors. J Nucl Med 2001; 42:213–21.

4. Hofmann M, Maecke H, Borner AR, et al. Biokinetics and imaging witht he somatostatin receptor PET radioligand 68Ga-DOTATOC: preliminary data. Eur J Nucl Med 2001;28:1751–7.

5. Henze M, Schuhmacher J, Hipp P, et al. PET imaging of somatostatin receptors using [68Ga]DOTA-D-Phe1-Tyr3-octreotide: first results in patients with meningiomas. J Nucl Med 2001;42:1053–6.

6. Lewis JS, Lewis MR, Cutler PD, et al. Radiotherapy and Dosimetry of ^{64}Cu-TETA-Tyr^{3}-Octreotate in a Somatostatin Receptor-positive, Tumor-bearing Rat Model. Clin Canc Res 1999;5:3608–16.

7. Anderson CJ, Jones LA, Bass LA, et al. Radiotherapy, toxicity and dosimetry of Copper-64-TETA-octreotide in tumor-bearing rats. J Nucl Med 1998;39:1944–50.

8. Lewis JS, Laforest R, Lewis MR, Anderson CJ. Comparative dosimetry of Copper-64 and Yttrium-90-labeled somatostatin analogs in a tumor-bearing rat model. Cancer Biother Radiopharm 2000;15: 593–604.

9. Breeman WAP, Mearadji A, Capello A, et al. Anti-tumor effect and increased survival after treatment with [^{177}Lu-DOTA^{0},Tyr^{3}]octreotate in a rat liver micrometastases model. Int J Cancer 2003;104:376–9.

10. Rogers BE, Zinn KR, Lin C-Y, Chaudhuri TR, Buchsbaum DJ. Targeted radiotherapy with [^{90}Y]-SMT 487 in mice bearing human nonsmall cell lung tumor xenografts induced to express human somatostatin receptor subtype 2 with an adenoviral vector. Cancer (Phila) 2002;94:1298–305.

11. Bodei L, Cremonesi M, Zoboli S, et al. Receptor-mediated radionuclide therapy with ^{90}Y-DOTATOC in assocation with amino acid infusion: a phase I study. Eur J Nuc Med 2003;30:207–16.

12. de Jong M, Breeman WAP, Bernard BF, et al. [^{177}Lu-DOTA^{0},Tyr^{3}]octreotate for somatostatin receptor-targeted radionuclide therapy. Int J Cancer 2001;92:628–33.

13. McCarthy DW, Shefer RE, Klinkowstein RE, et al. Efficient production of high specific activity Cu-64 using a biomedical cyclotron. Nucl Med Biol 1997;24:35–43.

14. Obata A, Kasamatsu S, McCarthy DW, et al. Production of therapeutic quantities of 64Cu using a 12 MeV cyclotron. Nucl Med Biol 2003;30:535–9.

15. Connett JM, Anderson CJ, Guo L-W, et al. Radioimmunotherapy with a Cu-64 labeled monoclonal antibody: A comparison with Cu-67. Proc Natl Acad Sci USA 1996;93:6814–8.

DOI:10.1158/1078-0432.CCR-04-1084

16. Lewis MR, Wang M, Axworthy DB, et al. In vivo evaluation of pretargeted Cu-64 for tumor imaging and therapy. J Nucl Med 2003; 44:1284–92.

17. Zimmermann K, Grunberg J, Honer M, et al. Targeting of renal carcinoma with Cu-64/67-labeled anti-L1-CAM antibody chCE7: selection of copper ligands and PET imaging. Nucl Med Biol 2003;30: 417–27.

18. Wu AM, Yazaki PJ, Tsai S, et al. High-resolution microPET imaging of carcinoembryonic antigen-positive xenografts by using a copper-64 engineered antibody fragment. Proc Natl Acad Sci USA 2000;97:8495–500.

19. Rogers BE, Bigott HM, McCarthy DW, et al. MicorPET imaging of a gastrin-releasing peptide receptor-positive tumor in a mouse model of human prostate cancer using a Cu-64-labeled bombesin analogue. Bioconjug Chem 2003;14:756–63.

20. Rogers BE, Anderson CJ, Connett JM, et al. Comparison of four bifunctional chelates for radiolabeling monoclonal antibodies with copper radioisotopes: biodistribution and metabolism. Bioconjug Chem 1996;7:511–22.

21. Bass LA, Wang M, Welch MJ, Anderson CJ. In vivo transchelation of Copper-64 from TETA-octreotide to superoxide dismutase in rat liver. Bioconjug Chem 2000;11:527–32.

22. Behr TM, Behe M, Sgouros G. Correlation of red marrow dosimetry with myelotoxicity: empirical factors influencing the radiation-induced myelotoxicity of radiolabeled antibodies, fragments, and peptides in pre-clinical and clinical settings. Cancer Biother Radiopharm 2002;17: 445–64.

23. Weisman GR, Wong EH, Hill DC, et al. Synthesis and transition-metal complexes of new cross-bridged tetraamine ligands. J Chem Soc Chem Commun 1996;947–8.

24. Wong EH, Weisman GR, Hill DC, et al. Synthesis and characterization of cross-bridged cyclams and pendant-armed derivatives and structural studies of their Copper(II) complexes. J Am Chem Soc 2000;122:10561–72.

25. Sun X, Wuest M, Weisman GR, et al. Radiolabeling and in vivo behavior of Copper-64-labeled cross-bridged cyclam ligands. J Med Chem 2002;45:469–77.

26. Jones-Wilson TM, Deal KA, Anderson CJ, et al. The in vivo behavior of Copper-64-labeled azamacrocyclic complexes. Nucl Med Biol 1998;25:523–30.

27. Boswell CA, Sun X, Niu W, et al. Comparative in vivo stability of copper-64-labeled cross-bridged and conventional tetraazamacrocyclic complexes. J Med Chem 2004;47:1465–74.

28. Rosewicz R, Vogt D, Harth N, et al. An amphicrine pancreatic cell line: AR42J cells combine exocrine and neuroendocrine properties. Eur J Cell Biol 1992;59:80–91.

29. Christophe J. Pancreatic tumoral cell line AR42J: an amphicrine model. Am J Physiol (Gastrointest Liver Physiol) 1994;266:G963–71.

30. Froidevaux S, Hintermann E, Torok M, et al. Differential regulation of somatostatin receptor subtype 2 (sst 2) expression in AR4–2J tumor cells implanted into mice during octreotide treatment. Cancer Res 1999; 59:3652–7.

31. Hofsli E, Thommesen L, Norsett K, et al. Expression of chromogranin A and somatostatin receptors in pancreatic AR42J cells. Mol Cell Endocrinol 2002;194:165–73.

32. Achilefu S, Wilhelm RR, Jimenez HN, Schmidt MA, Srinivasan A. A new method for the synthesis of tri-tert-butyl diethylenetriaminepentaacetic acid and its derivatives. J Org Chem 2000;65:1562–5.

33. Atherton E, Clive DL, Sheppard RC. Letter: Polyamide supports for polypeptide synthesis. J Am Chem Soc 1975;97:6584–5.

34. Edwards WB, Fields CG, Anderson CJ, et al. Generally applicable, convenient solid-phase synthesis and receptor affinities of octreotide analogs. J Med Chem 1994;37:3749–57.

35. Lewis JS, Srinivasan A, Schmidt MA, Anderson CJ. In vitro and in vivo evaluation of 64-Cu-TETA-Tyr3-Octreotate. A new somatostatin analog with improved target tissue uptake. Nucl Med Biol 1999;26: 267–73.

36. Wang M, Caruano AL, Lewis MR, et al. Subcellular localization of radiolabeled somatostatin analogues: implications for targeted radiotherapy of cancer. Cancer Res 2003;63:6864–9.

37. Li WP, Lewis JS, Kim J, et al. DOTA-D-Tyr^{1}-Octreotate: A somatostatin analogue for labeling with metal and halogen radionuclides for cancer imaging and therapy. Bioconjug Chem 2002;13:721–8.

38. Boswell CA, Sun X, Niu W, et al. In vivo stability of copper-64-labeled azamacrocyclic complexes: comparison of TETA and DOTA with cross-bridged chelators. J Med Chem. 2004; 47:1465–74.

39. Reubi JC, Schar J-C, Waser B, et al. Affinity profiles for human somatostatin receptor subtypes SST1-SST5 of somatostatin radiotracers selected for scintigraphic and radiotheraputic use. Eur J Nucl Med 2000;27:273–82.

40. O'Carroll A-M. Localization of messenger ribonucleic acids for somatostatin receptor subtypes (sstr1–5) in the rat adrenal gland. J Histochem Cytochem 2003;51:55–60.

41. Ludvigsen E, Olsson R, Stridsberg M, Janson ET, Sandler S. Expression and distribution of somatostatin receptor subtypes in the pancreatic islets of mice and rats. J Histochem Cytochem 2004;52: 391–400.

42. Koenig JA, Kaur R, Dodgeon I, Edwardson JM, Humphrey PPA. Fates of endocytosed somatostatin SST2 receptors and associated agonists. Biochem J 1998;336:291–8.

43. Akizawa H, Arano Y, Mifune M, et al. Effect of molecular charges on renal uptake of ^{111}In-DTPA-conjugated peptides. Nucl Med Biol 2001;28:761–8.

44. Akizawa H, Arano Y, Uezono T, et al. Renal metabolism of ^{111}In-DTPA-D-Phe-octreotide in vivo. Bioconjug Chem 1998;9: 662–70.

45. Bass LA, Lanahan MV, Duncan JR, et al. Identification of the soluble in vivo metabolites of Indium-111-diethylenetriaminepentaacetic acid-D-Phe^{1}-octreotide. Bioconjug Chem 1998;9:192–200.

46. Bernard BF, Krenning EP, Breeman WAP, et al. D-Lysine reduction of induim-111 octreotide and ytrium-90 octreotide renal uptake. J Nucl Med 1997;38:1929–33.

47. de Jong M, Rolleman EJ, Bernard BF, et al. Inhibition of renal uptake of indium-111-DTPA-octreotide in vivo. J Nucl Med 1996;37: 1388–92.